CRYSTAL STRUCTURES

R. Zallen

pp. 1-27 in *Handbook on Semiconductors, Volume One,* series edited by T.S. Moss, Volume One edited by W. Paul (North-Holland Publishing Company, Amsterdam, 1982).

CHAPTER 1

Crystal Structures

RICHARD ZALLEN

Xerox Webster Research Center
Webster, New York 14580
USA

Handbook on Semiconductors
edited by T. S. Moss
Volume 1, edited by W. Paul

Contents

1. Introduction and overview: The distribution of structures among the main semiconductor families

It is a fortunate fact that, among the most important families of semiconductor materials, a dominant role is played by a very small number of very simple and highly symmetric crystal structures. It might be argued that the overwhelming importance of silicon technology in the electronics industry could justify devoting nearly all of this chapter to a discussion of the diamond structure alone. That structure is illustrated in fig. 1, in a view through a large "ball-and-stick" model which forcefully brings home a sense of the long-range order (Pauling and Hayward 1964). A more conventional

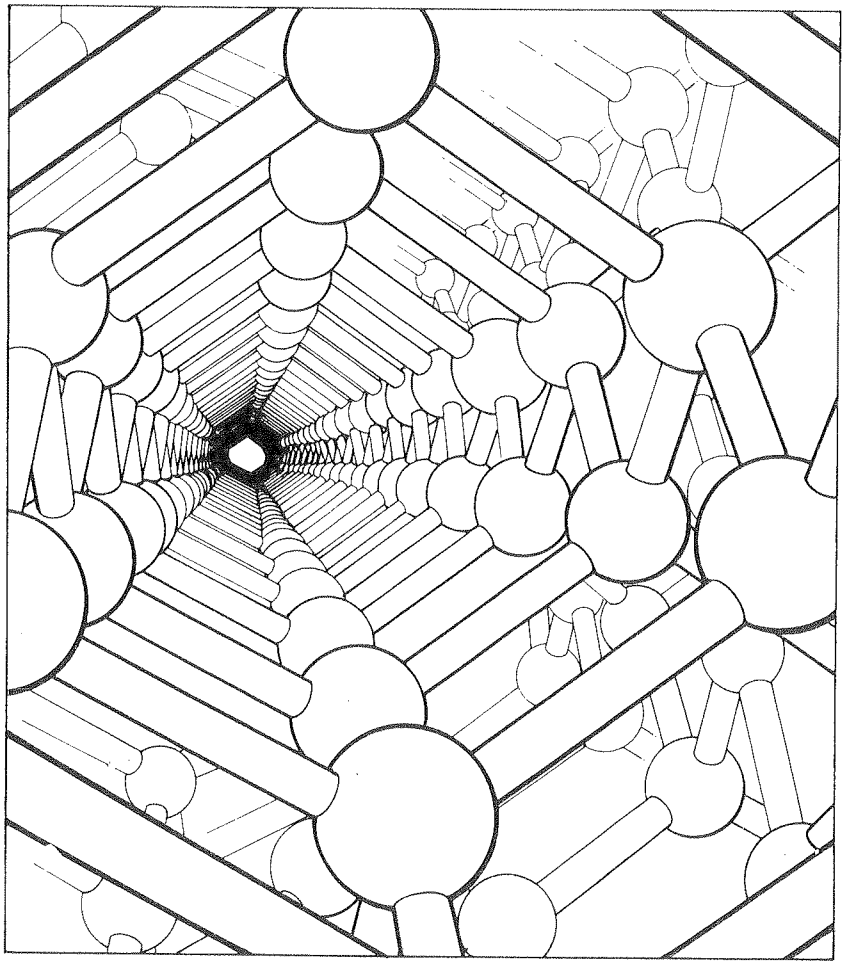

Fig. 1. Model of the diamond structure, viewed approximately along a (1, 1, 0) direction (adapted from a drawing in (Pauling and Hayward 1964)).

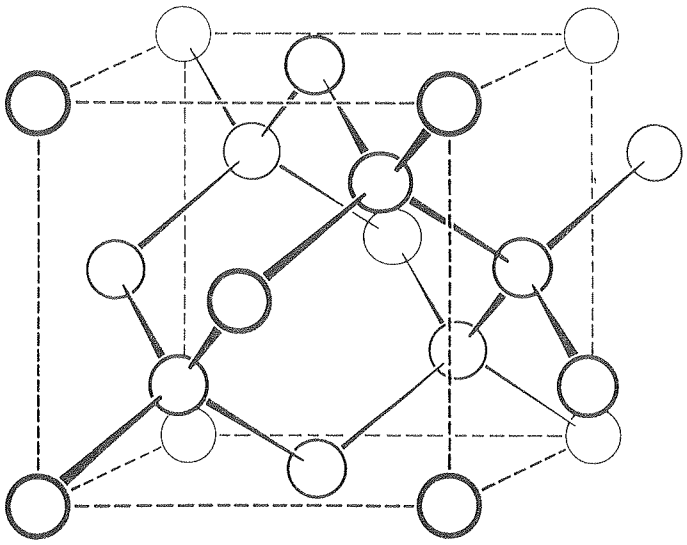

Fig. 2. The cubic unit cell of diamond.

diagram, showing a cubic unit cell, is shown in fig. 2. From a topological viewpoint, the diamond structure (with the atoms as "vertices" and the covalent bonds as "edges" of the topological "graph") is the *simplest* example of a *uniform four-connected three-dimensional network* (Wells 1977). Geometrically, with all bond lengths equal and with regular tetrahedral bond angles at the vertices, the diamond structure is also the *most symmetric embodiment* of the simplest 4-connected 3d network. Nature's reputed preference for simplicity is certainly not contradicted by the structure characteristic of the group IV solids: C, Si, Ge, and α-Sn.

Tetrahedral coordination is a hallmark of covalent semiconductors having eight valence electrons per pair of atoms. In addition to the elemental semiconductors of group IV (e.g. Si), this includes the A^nB^{8-n} families of binary compounds of types III–V (e.g. GaAs), II–VI (e.g. CdTe), and I–VII (e.g. AgI). Figure 3 displays the portion of the periodic table which contains the great majority of the elements which constitute the chemical components of semiconductor materials. Superimposed on the table are connections indicating examples of the binary families of compound semiconductors mentioned above. Closely related to the tetrahedrally-coordinated AB binaries are a host of more complex binaries (e.g. ZnP_2), ternaries (e.g. $CuInSe_2$), and quaternaries (e.g. Cu_2ZnGeS_4) which share the property of having the average number of valence electrons per atom equal to four. These complex tetrahedral structures, all of which can be regarded to be derived from the diamond structure, will not be discussed here; a systematic treatment has been given by Parthé (1964).

Figure 3 displays several "maps" which provide a graphic and compact representation of the distribution of crystal-structure types among the main families of semiconductors: the group IV elements and the AB compounds of types III–V, II–VI, I–VII, and IV–VI. The diatomic analog of the diamond structure (D) is the zincblende structure (Z) which is also cubic, though its symmetry is of course lower than that of diamond. Zincblende is the dominant structure type for the A^nB^{8-n} binaries, especially for the III–V compounds. Among the tetrahedrally-coordinated ($z = 4$) members of

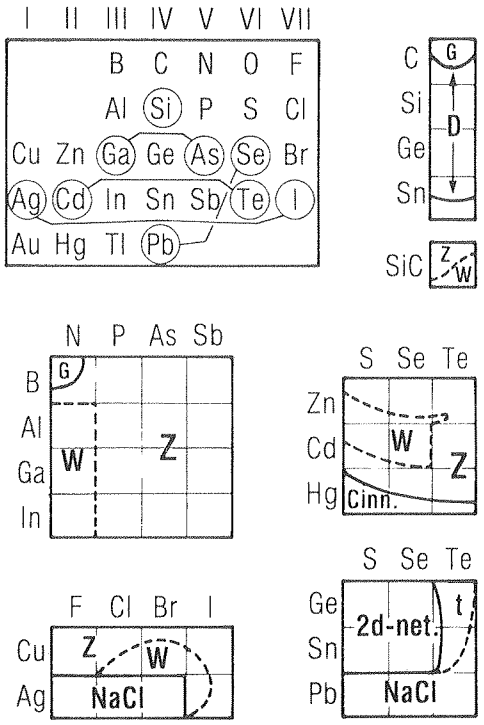

Fig. 3. The distribution of structures among the main semiconductor families. A typical representative of each family is indicated on the section of the periodic table shown at the top left. On the maps representing the distribution of structure types, solid boundaries separate structures with different coordinations while dashed boundaries separate structures with similar coordinations. The structure code is: D, diamond; Z, zincblende; W, wurtzite; NaCl, rocksalt; Cinn., cinnabar; and G, graphite or graphite-like. Other aspects are discussed in the text.

the II–VI and I–VII families, zincblende shares the field with the closely-related hexagonal-symmetry wurtzite structure (W). Octahedral coordination ($z = 6$) makes its appearance in the I–VII family in the form of the rocksalt structure (denoted in the figure by NaCl), and this structure also characterizes the lead-salt members of the IV–VI family, which has been included in fig. 3 as an important group of non-tetrahedral semiconductors. In all, about fifty chemically-distinct materials are included in fig. 3, and recognizing that different structures constitute physically-distinct solids substantially increases the number of materials represented.

Within the distribution maps of fig. 3, a solid line denotes a boundary between structures having different primary coordinations, while a dashed line denotes a boundary across which the primary coordination is unchanged. In some cases, boundaries have been drawn which cut through the square corresponding to a given substance. When this occurs, it means either that the material can exist at standard temperature and pressure in either of the designated structures, or it can be converted from one structure to the other by a *mild* departure from STP. If one structure is strongly preferred at STP, this is indicated in a schematic way by the dominant crystal form being given the lion's share of the box corresponding to the compound. To illustrate this, consider the case of the chalcogenides of mercury, which straddle the boundary between the zincblende and cinnabar structures (the latter will be described

in §3). HgS adopts the cinnabar structure at STP, but converts to zincblende above 300° C. HgSe and HgTe, on the other hand, have the zincblende form under normal conditions, but convert to the cinnabar form at modest pressures ($\sim$ 10 kbar). Thus, the zincblende/cinnabar boundary has been sketched to place most of the HgS square within cinnabar "territory" and most of the HgSe and HgTe squares within zincblende "territory". Although the position of the boundary indicates, in a qualitative way, the structural preference of the material, no quantitative interpretation should be placed upon its detailed location.

In constructing the structure-distribution maps of fig. 3, as well as in the other material collected in this review, several compilations of crystal-structure data have been used as the principal sources (Parthé 1964, Wyckoff 1962, Roth 1967, Hulliger 1976). These have been supplemented, in some cases, by later references in the primary literature. For example, the subtle situation found for SnTe has been sorted out only recently (Iizumi et al. 1975). This IV–VI semiconductor, along with GeTe, exhibits a trigonal modification (corresponding to the strip labelled *t* in fig. 3) which is an extremely slight distortion of the rocksalt structure. To complete the structures found in the IV–VI family, the area labelled "2d-net." marks the occurrence of a layer-structure (two-dimensional network (Zallen 1974, 1975)) crystal form (Hulliger 1976).

Four simple structures dominate the distributions of fig. 3: diamond, zincblende, wurtzite, and rocksalt. Zincblende alone is exhibited by nearly thirty materials. This chapter will concentrate mainly on these four structures, discussing them in some detail. Not, however, to the exclusion of other less-common crystalline forms. Semiconducting solids are characterized by covalent bonding, and covalent bonding is accompanied by low coordination numbers. Open structures and low filling factors result. This allows for a great deal of freedom in building up the crystal structure, in contrast to the close-packed structures which occur for metallic and highly-ionic crystals. It is important to convey an impression of the great diversity of forms available to crystalline semiconductors, and one section of this chapter will be set aside for this purpose.

Section 2 assembles information about the symmetry properties of the dominant structures of fig. 3. A quick survey of a variety of other crystals, including chain-structure and layer-structure semiconductors, is given in §3. In §4 we return to the principal structures, especially zincblende and wurtzite, with a description of geometric and topologic features, polytypism, lattice constants, and Brillouin zones. Section 5 contains a few examples of spectroscopic consequences of structure and symmetry.

2. Symmetry properties of the principal structures

The "principal structures" from the semiconductor viewpoint are diamond, zincblende, wurtzite, and rocksalt. (In the venerable Strukturbericht notation, these are A1, B3, B4, and B1, respectively.) The diamond structure has already been shown, and its diatomic analog–zincblende– will be shown in §4. The other key tetrahedral structure, wurtzite, is shown in fig. 4, and the familiar rocksalt structure is shown in fig. 5.

A large amount of information about symmetry (and some other) properties of these

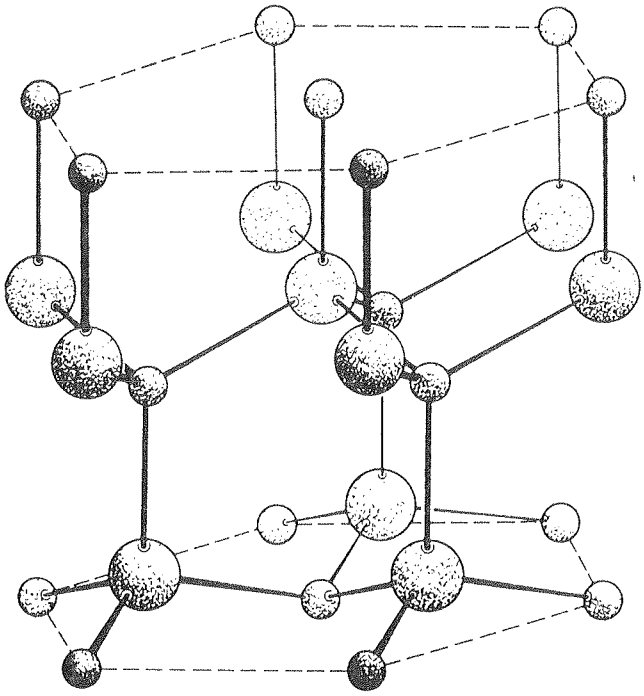

Fig. 4. The wurtzite structure.

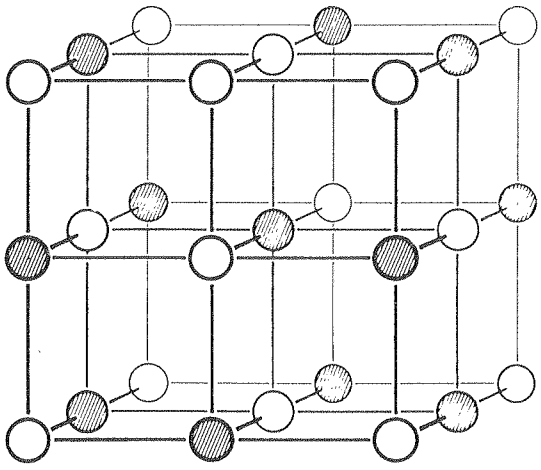

Fig. 5. The rocksalt structure.

structures is presented in table 1. This table also includes information about a few other structures in order to set up a bridge to the following section. However, in the present section we shall focus on the "big four", discussing the information contained in the first four rows of table 1.

For each structure, the prototype listed in the second column of the table is a material whose primary form at STP is the structure under consideration. The coordination number is the number of nearest-neighbor atoms, the most important single parameter characterizing the local bonding in the solid. Network dimensionality, listed in the fourth column, is a crucial *topological* characterization of the network formed by the

Table 1
Structures and crystal symmetries of the simplest and most important semiconductor families.

Structure	Prototype	Coordination	Network dimensionality	Atoms per prim. cell	Order of the factor group	Crystal class	Triperiodic space group	Lattice	Atomic positions	Site symmetry	Bonding anisotropy $(r_1/r_0)-1$
Diamond	Si	4	3d	2	48	cubic	Fd3m (O_h^7) No. 227	fcc	0, 0, 0; 1/4, 1/4, 1/4.	$\bar{4}3m$ (T_d)	0
Zincblende	GaAs	4	3d	2	24	cubic	F$\bar{4}$3m (T_d^2) No. 216	fcc	diatomic analog of Si	$\bar{4}3m$ (T_d)	0
Wurtzite	CdSe	4	3d	4	12	hexagonal	$P6_3mc$ (C_{6v}^4) No. 186	hex.	Cd: 0, 0, 0; 1/3, 2/3, 1/2. Se: add 0, 0, u to above ($u \approx 3/8$)	3m (C_{3v})	0
Rocksalt	PbS	6	3d	2	48	cubic	Fm3m (O_h^5) No. 225	fcc	0, 0, 0; 1/2, 1/2, 1/2.	m3m (O_h)	0
Distorted rocksalt	GeTe	6(3)	3d(2d)	2	6	trigonal	R3m (C_{3v}^5) No. 160	(fcc)′	δ, δ, δ; $\delta \approx 0.02$ $\delta', \delta', \delta'$; $\delta' = (1/2)-\delta$	3m (C_{3v})	0.1
Cinnabar	HgS	6(2)	3d(1d)	6	6	trigonal	$P3_121$ (D_3^4) No. 152	hex.	diatomic analog of Se	2 (C_2)	0.35
Chain	Se	2(6)	1d(3d)	3	6	trigonal	$P3_121$ (D_3^4) No. 152	hex.	u, 0, 0; 0, u, 1/3; u, u, 2/3, $u \approx 0.2$	2 (C_2)	0.45

atoms and their pairwise connections (the covalent bonds). It is the number of dimensions in which the covalently connected network is indefinitely extendable, i.e. it is the *macroscopic dimensionality* of the molecular (or macromolecular) covalently bound unit (Zallen 1974). The four main structures are all 3d networks, but there are other structures exhibited by semiconducting solids (some of which are discussed in the next section) which have lower network dimensionalities.

The next seven columns of table 1 specify the key characteristics of the crystal symmetry. The notation and terminology adopted here follows that of the definitive International Tables for X-ray Crystallography (Henry and Lonsdale 1976). Although a few definitions will be given, and others will be evident from the context, it is impractical to attempt a short course in crystallography in this chapter. The reader is referred to the International Tables and to the texts by Buerger (1963) and Megaw (1973). For group-theoretical methodology many good source works are available, including the books by Jones (1960) and Lax (1974).

It is instructive to view the fifth and sixth columns of the table as measures, respectively, of crystal complexity (atoms per primitive cell, the smallest unit from which the crystal may be constructed via translation) and of crystal symmetry (order of the factor group, the number of distinct generalized rotations which transform the structure into itself). The disparity between these columns reflects the degree to which nature has been kind to us in the simplicity of the main structures. In each instance, the primitive-cell size (2 for the cubic structures, 4 for wurtzite) is far outstripped by the size of the factor group. For diamond and rocksalt the latter is 48, which is the maximum value possible for a three-dimensional crystal. This happy situation greatly simplifies theoretical analyses of these solids. In the following section, we will meet cases in which the complexity/symmetry "ratio" is reversed, and life is less simple.

Three equivalent labels are tabulated for the crystal space group: the international "short symbol", the older but still widely-used Schoenflies symbol, and the number of the space group in the systematic listing of the International Tables (Henry and Lonsdale 1976). The Bravais lattice for the three cubic structures is face-centered cubic, (defined in §4.1), and for wurtzite it is the hexagonal lattice. Coordinates of atomic positions are given with respect to the cubic (nonprimitive) unit cell for diamond, zincblende, and rocksalt, in units of the cube edge. Hexagonal coordinates of the conventional type (Henry and Lonsdale 1976, Buerger 1963, Megaw 1973, Jones 1960) are used for wurtzite (look ahead to fig. 16). Site symmetry, the point-group symmetry about each atomic site, is given in the next-to-last column of the table in both international and Schoenflies notations.

The last column of table 1, the bonding anisotropy defined as $(r_1/r_0)-1$, does not refer to a quantity determined by symmetry. It is essentially a geometric measure of a force constant, or intramolecular/intermolecular interaction ratio relevant to a molecular crystal, i.e. a crystal characterized by the coexistence of strong (intramolecular, typically covalent), and weak (intermolecular, typically van der Waals) interatomic interactions. Here r_0 is the covalent bond length and r_1 is the closest atom–atom separation between molecules. For a 3d-network solid, the bonding anisotropy vanishes, but for molecular solids it provides a measure of the de-coupling between the low-dimensionality networks. It differs from zero for the three structures

described in the lower part of table 1, and these three introduce the discussion of diversity which is given in the following section.

3. A spectrum of structures

Our point of departure for the foray into a sampling of other notable semiconductor structures is the rocksalt structure of fig. 5, because several structures may be viewed as lesser or greater distortions of rocksalt. First, it should be remarked that a generous definition of the term "semiconductor" is being employed in this chapter in order to provide a broad perspective, and also in order to include a few prototypical structures in this particular section. Although most of the materials included in the main families of fig. 3 fall within a conventional semiconductor category (say, bandgap between 0 and 3 eV), note that even those predominantly semiconductor groups include insulators and semimetals (e.g. the diamond and graphite forms of C, respectively). The zincblende-structure mercury chalcogenides, as well as α-Sn, are zero-gap semiconductors (Groves and Paul 1963, Lovett 1977).

We begin within the IV–VI family, examining the tellurides. PbTe, like the other lead salts, has the rocksalt structure. For SnTe and GeTe, a new ferroelectric structure appears (it is the form adopted by SnTe at low temperature and by GeTe at STP) which is a very slight trigonal distortion of rocksalt (Hulliger 1976, Iizumi et al. 1975). The GeTe structure can be derived from rocksalt by a small displacement of the Ge and Te sublattices, with respect to each other, along a (1, 1, 1) direction. Symmetry properties of this structure have been included in table 1. Note the entries 6(3) and 3d(2d) for its coordination and network dimensionality, respectively. The sixfold coordination of rocksalt has been replaced by a situation in which three neighbors are slightly closer and three are slightly further away than originally. The appropriate view of GeTe, with respect to network dimensionality, is to ignore the slight difference in nearest-neighbor spacings, and to treat it as a 3d-network solid of coordination 6. If the difference were taken seriously, then the quantities in parentheses would apply: coordination 3 and network dimensionality 2d. The corresponding bonding anisotropy is about 0.1 at room temperature; it varies smoothly to zero at the second-order trigonal → cubic displacive transition to the rocksalt form.

The cinnabar form of the mercury salts HgS, HgSe and HgTe can also be derived from rocksalt by a trigonal distortion, but a more severe one than for GeTe. Cinnabar is described in table 1 and its unit cell is illustrated in fig. 6a. The strong bonds define a –S–Hg–S–Hg– helical chain, a 1d network. Figure 6b shows a planar projection which indicates the distorted-rocksalt aspect (Zallen et al. 1970); nearest-neighbor covalent bonds (r_0) are denoted by heavy lines, second-neighbor "interchain" bonds (r_1) are denoted by light lines. Although the bonding anisotropy is now quite substantial, the appreciable ionic contribution to the interchain bonding in HgS causes this crystal to more-closely resemble a 3d-network solid than a 1d-network solid (Zallen et al. 1970).

If one envisages cinnabar with the Hg atoms removed and the sulfurs replaced by Se atoms, then the result is essentially that of trigonal Se (fig. 7), a very simple and important structure which is the last one listed and described in table 1. This is the

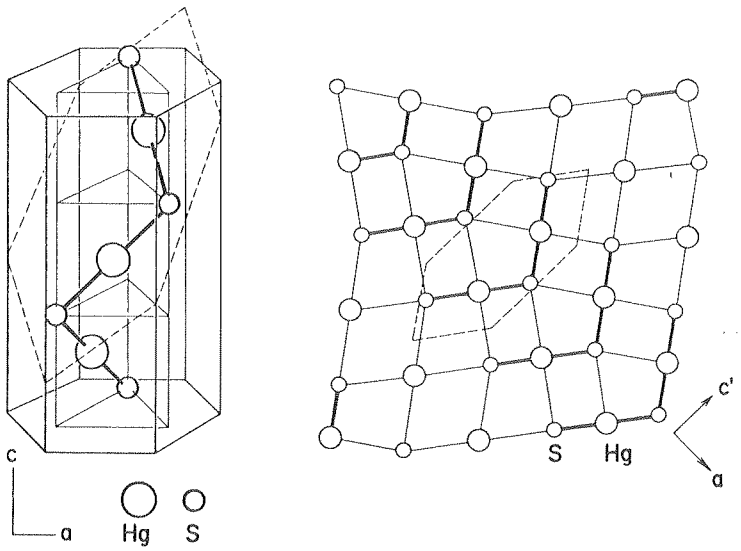

Fig. 6. The cinnabar structure: (a) the primitive cell, (b) projection on the plane shown dashed in (a) (Zallen et al. 1970).

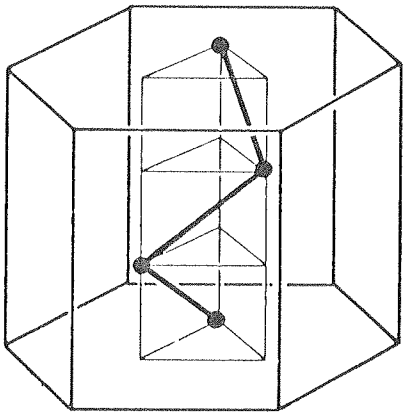

Fig. 7. The primitive cell of the structure of trigonal Se.

primary form of the two group VI semiconductors Se and Te. Just as cinnabar may be derived by a trigonal distortion of rocksalt, so it is possible to derive the selenium structure via a large trigonal distortion of the simple cubic structure. (Metallic polonium, the group VI element in the row below Te, actually crystallizes in a simple cubic form.)

Se and Te are the simplest polymers. These elemental crystals are essentially 1d-network solids made up of helical chains in hexagonal array (close packing for rods). Within each helix there are three atoms per turn. From table 1 it can be seen that the bonding anisotropy is greater than for HgS, and in Se the interchain coupling lacks an ionic component and is essentially of the weak van der Waals type. Thus this crystal may appropriately be viewed as a 1d-network solid, a molecular solid made up of long-chain macromolecules.

Se and Te are notable as the simplest elemental crystals to display reststrahlen bands, i.e., to possess lattice vibrations which are infrared active in first order. This aspect, in which they differ greatly from the elemental semiconductors of the germanium family, is explained in the last section of the chapter. It should also be noted that because they are based on helical sub-units, all of which have the same "handedness," both right-handed and left-handed crystal forms exist. Table 1 describes (and fig. 7 shows) the right-handed form; the enantiomorphic left-handed form has space group $P3_221$ (D_3^6). This also applies to the cinnabar structure. The three-atom unit cell of Se and Te is the minimum needed to define a helix, and these two crystals are the simplest ones to exhibit circular dichroism and optical activity.

We now proceed to less simple structures, surveying these by way of the crystals characterized in table 2. This table differs from the first in two respects:

(1) atomic positions and site symmetries are omitted;

(2) a second symmetry (in addition to the crystal symmetry) is specified, which refers to a single molecular or macromolecular unit.

The first change is necessitated by the large unit cells of most of these structures. Site symmetries are typically low; in the second half of table 2, no atom is taken into itself by *any* operation (other than the identity) of the crystal factor group.

Change (2) is the significant one. The appearance of a second distinct symmetry, which coexists and competes with the crystal symmetry, is characteristic of crystals in which the network dimensionality is 0, 1, or 2 (Zallen 1974, 1975). The symmetry of the restricted-dimensionality covalent network is the generalization of molecular symmetry, and in many cases it is the *dominant* symmetry in determining physical properties (a spectroscopic example is given in § 5). Note that the molecular group is, in general, not a subgroup or a supergroup of the crystal factor group. Comparing the orders of the two groups, as given in the sixth and eleventh columns of table 2, reveals that the molecular symmetry can be either higher (e.g. As_4S_4) or lower (e.g. GaS), or of the same order (e.g. PbI_2) as the crystal symmetry.

Molecular crystals of the most familiar type are those in which the covalent network is finite on an atomic scale, termed 0d-network solids in our classification. These are represented in table 2 by two chalcogenide crystals based on eight-atom molecules: orthorhombic sulfur in which the molecule is an S_8 ring, and realgar (Mullen and Nowacki 1972) in which the molecule is an As_4S_4 cage. The molecular symmetry (tetragonal for these two examples) is a point-group symmetry for a 0d-network crystal.

The simplest 1d-network crystal was already introduced in table 1. Trigonal Se is an example of a case in which the molecular and crystal symmetries are essentially similar in the sense that the crystal space group can be generated from the group of a single chain (which is now a space group because it includes not only rotations but also pure translations parallel to the chain) simply by the addition of translations perpendicular to the chain. This can occur when the crystal primitive cell contains just a single primitive cell of the chain, i.e., when the translational repeat units of crystal and chain coincide. A similar situation can occur for 2d-network crystals when there is "one molecule per unit cell" in the same sense – the crystal primitive cell contains the same atomic configuration as the primitive cell of the extended layer. An example is the PbI_2 structure included in table 2. In the above, the primitive cell of the chain (layer) is

Table 2
Structures, crystal symmetries, and molecular (or macromolecular) symmetries of less-simple semiconductor crystals.

Structure	Prototype	Coordination	Network dimensionality	Atoms per prim. cell	Order of the crystal factor group	Crystal class	Triperiodic space group	Molecules per prim. cell	Point group or factor group symmetry of the isolated molecule or macromolecule	Order of the molec. point or factor group	Bonding anisotropy $(r_1/r_0)-1$
Layer (dist. NaCl)	GeSe	3	2d	8	8	orthorhombic	Pnma (D_{2h}^{16})	2	DG 32 (C_{2v}^{7})	4	0.3
Graphite	C	3	2d	4	24	hexagonal	$P6_3/mmc$ (D_{6h}^{4})	2	DG 80 (D_{6h}^{1})	24	1.35
Layer	BN	3	2d	4	24	hexagonal	$P6_3/mmc$ (D_{6h}^{4})	2	DG 78 (D_{3h}^{1})	12	1.3
Layer	GaS	4, 2	2d	8	24	hexagonal	$P6_3/mmc$ (D_{6h}^{4})	2	DG 78 (D_{3h}^{1})	12	0.6
Layer	PbI_2	6, 3	2d	3	12	trigonal	$P\bar{3}ml$ (D_{3d}^{3})	1	DG 72 (D_{3d}^{3})	12	0.4
Ring molecule	S_8	2	0d	32	8	orthorhombic	Fddd (D_{2h}^{24})	4	$\bar{8}2m$ (D_{4d})	16	0.8
Cage molecule	As_4S_4	3, 2	0d	32	4	monoclinic	$P2_1/n$ (C_{2h}^{5})	4	$\bar{4}2m$ (D_{2d})	8	0.55
Orpiment	As_2S_3	3, 2	2d	20	4	monoclinic	$P2_1/n$ (C_{2h}^{5})	2	DG 32 (C_{2v}^{7})	4	0.55
Layer	$GeSe_2$	4, 2	2d	48	4	monoclinic	$P2_1/n$ (C_{2h}^{5})	2	DG 32 (C_{2v}^{7})	4	0.6
Quartz-like	GeS_2	4, 2	3d	36	2	monoclinic	Pc (C_{1h}^{2})	–	–	–	0

defined as the smallest unit which suffices to generate the macromolecule by one-dimensional (two-dimensional) translations.

Layer-structure (2d-network) semiconductors occur in great variety (Hulliger 1976), and it is this class which is most representative of the diversity available to semiconductor structures. For this reason, graphite, the archetype 2d-network solid, has been included in table 2 (in spite of the fact that it is, of course, a semimetal). Graphite is elemental, has the largest bonding anisotropy (i.e. is the most "layerlike"), and has the highest symmetry available to a layer crystal. In a 2d-network crystal, the molecular symmetry is a diperiodic space group, the symmetry applicable to a three-dimensional object which has translational periodicity in two dimensions. There are 80 such diperiodic groups (DG), and their relationship to other more familiar groups (such as the 230 crystallographic space groups) is schematically indicated in fig. 8. Although the DG layer symmetry is not normally explicitly listed in the crystal-structure report for a layer crystal, it may readily be derived for a given layer structure with the aid of the systematic listing and description of the diperiodic groups given by Wood (1964). The DG numbers used in table 2 follows Wood's notation.

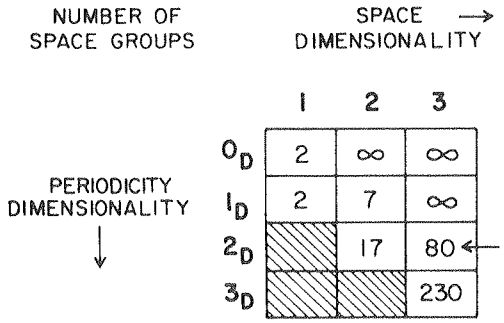

Fig. 8. The relationship of the 80 diperiodic groups to other types of space and point groups. The diperiodic groups are essential to the understanding of the properties of 2d-network (layer-structure) semiconductors.

Of the 2d-network semiconductor structures described in table 2, two are illustrated in figs. 9 and 10. The beautiful pattern shown in fig. 9 represents a view normal to one layer in PbI_2*. This simple and symmetric 2d-network consists of an I–Pb–I three-plane sandwich in which each lead atom is bonded to six iodines and each iodine to three leads. Many transition-metal dichalcogenides, such as TaS_2, crystallize in this structure.

Figure 10 presents the structure of orpiment, crystalline As_2S_3 (Mullen and Nowacki 1972, Zallen et al. 1971). Orpiment is notable as the layer crystal for which the crucial role of the diperiodic symmetry was first appreciated and analyzed (Zallen et al. 1971). The dominance of the layer symmetry (and, conversely, the minor subsidiary role of the triperiodic crystal symmetry) in determining the optical properties of As_2S_3 is briefly described in § 5. Orpiment, as well as the isomorphic crystal As_2Se_3, have also served as

* This is the crystal structure of 2H–PbI_2, the simplest (one layer per unit cell) and predominant polytype of PbI_2. It is sometimes referred to as the cadmium iodide structure, and it is the same as the structure which among the layered dichalcogenides is known as the 1T–TaS_2 structure.

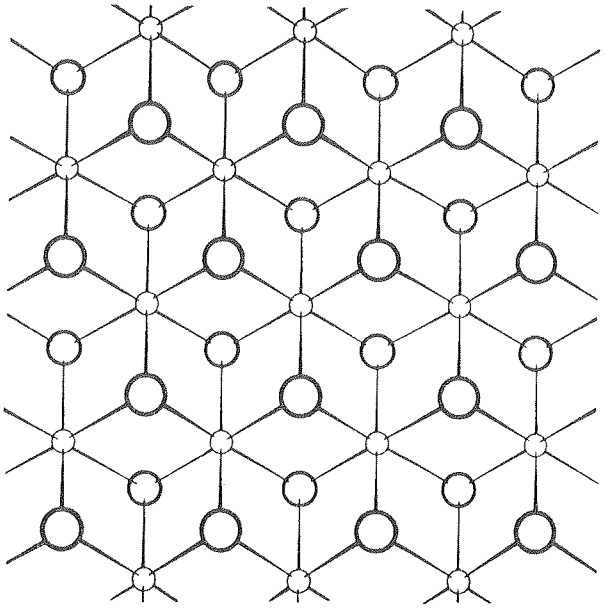

Fig. 9. A single layer in the PbI_2 structure.

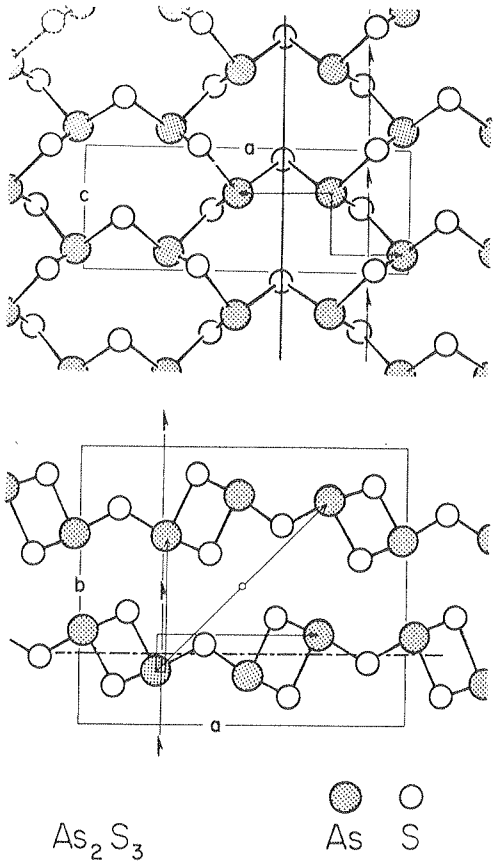

As_2S_3

Fig. 10. Crystal structure of As_2S_3 and As_2Se_3, the orpiment structure. The bottom diagram shows a view along the *c*-axis, looking at the layers edge on; the top diagram shows a view along the *b*-axis, looking down on a single layer. Crystal-symmetry operations are indicated on the former, layer-symmetry operations on the latter (Zallen et al. 1971).

valuable crystalline analogs of the important chalcogenide glasses of the same chemical composition and short-range order. (Amorphous As_2S_3 and As_2Se_3 are bulk glasses of technological significance as infrared-transmitting window materials and as visible-sensitive large-area photoconductors.)

For orpiment, both the crystal and the layer factor groups are of order 4, and the small number of symmetry operations present have all been shown in fig. 10. The three monoclinic crystal-symmetry operations are shown in the lower part of the figure (the fourth operation is the identity). Two operations of the orthorhombic layer symmetry are shown in the upper part of the figure (the other two are the identity and the glide plane which the layer and crystal symmetries have in common). Notice how different the two symmetries are: The crystal possesses a center of symmetry while an individual layer does not; the layer possesses a mirror plane normal to the *a*-axis while the crystal lacks this. These differences permit a clear test of the competition between the two symmetries, since they imply experimentally distinguishable optical properties. The data, as explained in §5, demonstrate the dominance of the layer symmetry. The orthorhombic diperiodic space group applicable to the layer in orpiment, DG 32 (closely related, as described by Wood (1964), to the triperiodic group C_{2v}^7), also applies to two other structures listed in table 2.

To end this survey, we return, in the last entry of table 2, to a 3d-network crystal. GeS_2 exhibits two crystalline forms. One of these is a layer structure which is isomorphic to the $GeSe_2$ structure described in the next-to-last row of the table (Dittmar and Schafer 1975, 1976a). The other is the 3d-network structure described in the last row (Dittmar and Schafer 1976b). The complexity/symmetry balance for this complex structure, 36 atoms per primitive cell versus a crystal factor group containing merely 2 operations, is the reverse of that which we noted earlier for the cubic structures of table 1. While for diamond and zincblende and, for that matter, for such simple and relatively symmetric structures as Se and PbI_2, symmetry alone is sufficient to determine the long-wavelength vibrational eigenvectors, group theory is of little help in the analysis of a crystal such as GeS_2. In this respect, the combination of high unit-cell complexity and low crystal symmetry simulates the situation in an amorphous solid. GeS_2 can, in fact, easily be prepared in solid form as a bulk glass.

4. Diamond, zincblende, wurtzite, and rocksalt

4.1. General properties

In this section we treat in more depth the four principal structures which dominate fig. 3, focussing especially on the tetrahedral structures diamond, zincblende, and wurtzite. The main structural and symmetry properties of the four have been described previously in table 1.

The cubic structures of diamond and rocksalt have been shown in figs. 3 and 5; that of zincblende is shown in fig. 11. (Sphalerite is another name sometimes used for zincblende.) All three share the same translational symmetry, which corresponds to the face-centered cubic Bravais lattice of fig. 12 (Ziman 1963). The atomic positions given in

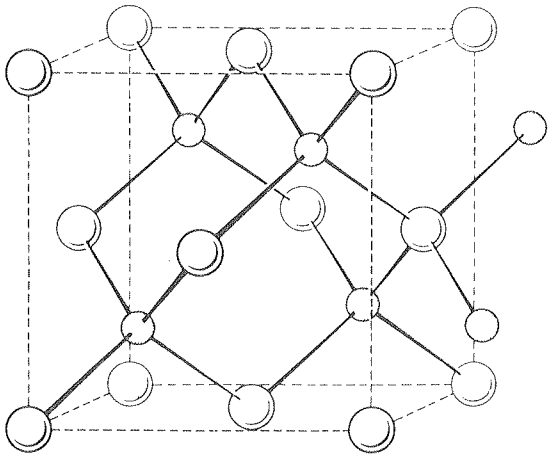

Fig. 11. The zincblende structure.

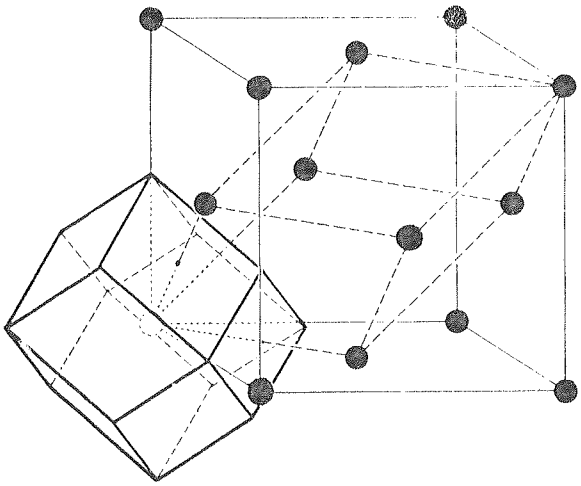

Fig. 12. The face-centered cubic lattice showing the cubic unit cell, the parallelepiped primitive cell of the Bravais lattice (shown dashed), and the Wigner–Seitz primitive cell (Ziman 1963).

table 1 are in units of the edge of the unit cube of fig. 12. The base vectors of the fcc translation group are given in the top of table 3, in which a denotes the cube edge.

The unit cube contains four translational repeat units, i.e. four primitive cells. Two choices of primitive cell are shown in fig. 12: the usual parallelepiped unit cell (shown dashed), and the rhombic dodecahedron (shown in solid outline) which is the Wigner–Seitz cell of the fcc lattice. Both contain two atoms, positioned as stated in table 1. Comparing figs. 11 and 12 shows that either sublattice in the zincblende structure (say, the Ga sublattice in GaAs) defines an fcc lattice. Rocksalt has the same property.

Sections 4.2 and 4.3 are devoted to the tetrahedral structures: §4.2 describes their local geometry and topology, and §4.3 deals with polytypism (structures "intermediate" between zincblende and wurtzite). Section 4.4 collects a listing of lattice constants of the semiconductors which crystallize in the four principal structures, and

Table 3
Primitive translation vectors for the face-centered cubic translation group, base vectors of the corresponding reciprocal lattice, and some special points of high symmetry in the Brillouin zone (applicable to the diamond, zincblende, and rocksalt structures).

Real-space lattice vectors	$a_1 = (1, 1, 0)(a/2)$			
	$a_2 = (1, 0, 1)(a/2)$			
	$a_3 = (0, 1, 1)(a/2)$			
Reciprocal-space lattice vectors	$b_1 = (1, 1, -1)(2\pi/a)$			
	$b_2 = (1, -1, 1)(2\pi/a)$			
	$b_3 = (-1, 1, 1)(2\pi/a)$			
Symmetry points in the Brillouin zone	Γ	(0, 0, 0)	multiplicity	1
	X	$(1, 0, 0)(2\pi/a)$		3
	L	$(1/2, 1/2, 1/2)(2\pi/a)$		4
	Δ	$(k, 0, 0)$		6
	Λ	(k, k, k)		8
General point	k	(k_1, k_2, k_3)		48

§4.5 describes their Brillouin zones. To supplement the group-theoretical information contained in this chapter, we call attention to the detailed treatment which has been given by Birman (1974) for the cubic semiconductor structures.

4.2. Local geometry and topology

The tetrahedral coordination in diamond, zincblende, and wurtzite is evident in figs. 1, 2, 4, and 11. The four nearest-neighbor bonds are equal, and each pair of bonds meet at a bond angle of 109°. This tetrahedral environment is symmetry determined in diamond and zincblende. In wurtzite, because it is hexagonal rather than cubic, one bond is permitted to differ in length from the other three and the bond angles may deviate from the tetrahedral value. However, the deviation from tetrahedral in wurtzite-structure crystals is found to be very small (see §4.4). The site symmetries at the atomic positions were given in table 1: tetrahedral (T_d) in diamond and zincblende, trigonal (C_{3v}) in wurtzite.

The tetrahedral coordination is itself the single most important parameter of the short-range order in these crystals. Beyond nearest neighbors, other topological and geometric parameters may be specified to characterize the local order in these structures, and several sets are presented in table 4.

The upper part of table 4 specifies the characteristics of the first few shells of atoms surrounding any given atom in diamond, zincblende, and wurtzite. All neighbors within a distance of 2.5 bond lengths have been included (34 neighbors in all for diamond/zincblende, 38 for wurtzite). Zincblende and wurtzite have the same number and type of second neighbors (12 of type A, where the origin is an atom of chemical species A), just as they do for first neighbors (4 of type B). They differ for third neighbors, and beyond. Note the close third neighbor in wurtzite; it is located along the

Table 4
Local topology and geometry of the zincblende, diamond (same as zincblende, with A = B), and wurtzite structures.

Number of bond "steps" from the initial atom (chemically of type A)	Distance from the initial atom (in units of bond length)	Chemical species of the neighboring atom	Number of neighbors of the specified type	
			Zincblende	Wurtzite
1	1.0	B	4	4
2	$(8/3)^{1/2} = 1.633$	A	12	12
3	$5/3 = 1.667$	B	–	1
3	$(11/3)^{1/2} = 1.915$	B	12	9
4	$(16/3)^{1/2} = 2.309$	A	6	6
3	$7/3 = 2.333$	B	–	6
Fraction of bonds in the *staggered* configuration			1	3/4
Fraction of bonds in the *eclipsed* configuration			0	1/4
Fraction of six-atom rings in the *chair* configuration			1	1/4
Fraction of six-atom rings in the *boat* configuration			0	3/4
Number of 6-rings which pass through each atom			12	12
Number of 8-rings which pass through each atom			24	24

same trigonal axis that passes through the origin atom and is removed from it by a short diameter of a "boat-shaped" six-atom ring (see below).

The next entry in table 4 describes the relative orientation of adjacent tetrahedra, tetrahedra which share one bond. Figure 13 shows what is meant by the "eclipsed" and "staggered" configurations. The angular variable at issue, which refers to the relative disposition of second-neighbor bonds (rather than nearest-neighbor bonds, whose relative orientation is given by the bond angle), is called the dihedral angle. This is the angle which separates the two trios of bonds of adjacent tetrahedra, when they are

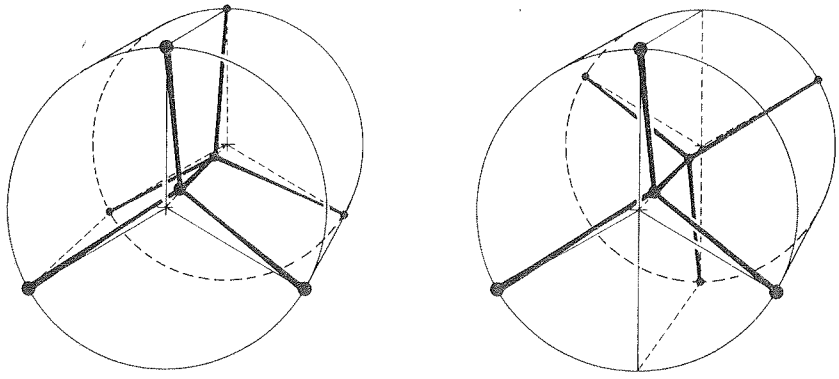

Fig. 13. The eclipsed and staggered bond configurations in tetrahedral semiconductors.

projected upon the plane perpendicular to the shared bond. Only the staggered configuration (dihedral angle of 60°) occurs in zincblende; in wurtzite, $\frac{3}{4}$ of the bonds are in the staggered configuration and $\frac{1}{4}$ are in the eclipsed configuration (dihedral angle of zero).

Topologically, an important characteristic of a network is the shortest circuit (closed loop or n-ring consisting of n adjacent bonds, n connected sites) that it contains. In both zincblende and wurtzite, the shortest circuit is $n = 6$. Every atom belongs to 12 distinct 6-atom rings. Geometrically, the 6-rings are of one type in zincblende, two types in wurtzite, as stated in table 4. The "boat" and "chair" configurations are shown in fig. 14.

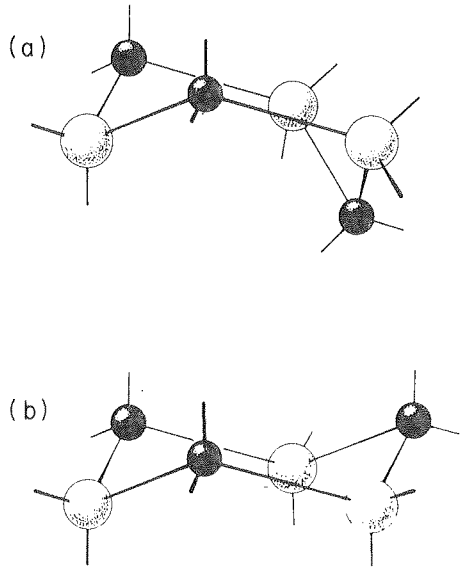

Fig. 14. The boat (a) and chair (b) configurations of six-atom rings.

It should be noted that in amorphous solids, symmetry characterizations disappear, but short-range considerations (such as those given in table 4) continue to apply. The structure of amorphous silicon is tetrahedrally coordinated and is characterized by a continuous distribution of dihedral angles which spans all values between those corresponding to the staggered and eclipsed configurations. While diamond and the other tetrahedral crystal structures contain only even-membered rings, odd-membered rings occur in amorphous silicon in which the shortest circuits are believed to be 5-rings.

4.3. Polytypism

The intimate connection between the zincblende and wurtzite structures has been noted previously and is evident from table 4. As seen in fig. 3, many compounds in the II–VI and I–VII families readily crystallize in both structures. In fact ZnS, as well as the IV–IV compound SiC, crystallize not only in both structures but also in a large number of structures which are "in-between" the two.

The underlying geometrical basis for this phenomenon may be understood in terms of a familiar problem phrased in terms of the large number of ways of optimally filling

space with equal spheres. A first layer of spheres is arranged, with their centers coplanar, in two-dimensional close packing (a triangular lattice, each sphere contacts six neighbors along a horizontal equator). There are now two ways to lay down a second like layer to nest on the first so that each sphere of the second layer touches three spheres of the first. Label the horizontal position of the first layer as A, that chosen for the second layer as B, and the unused second-layer position as C. (For a view of the relative positions of the projections of layers A, B, C on a horizontal plane, note the upper and lower iodine atoms and the lead atoms shown in fig. 9.) The third layer can now be placed above the second at C or A. If C is used, the fourth can go at A or B, and so on. There are always two choices for each additional layer, so that there exists an unlimited variety of layer sequences which fill space equally well. In each case, every sphere contacts 12 others: 6 in the same layer, 3 in the layer "below," and 3 in the layer "above."

The layer sequence ABCABCABC . . . corresponds to cubic close packing; the sphere centers form a fcc lattice with the vertical axis a (1, 1, 1) axis. The sequence ABABABAB . . . corresponds to hexagonal close packing; the sphere centers form a hcp lattice with the c-axis vertical. Now if we examine, say, the Zn sublattice in zincblende ZnS, we find the fcc lattice, while the Zn sublattice in wurtzite ZnS forms the hcp lattice. Just as the zincblende and wurtzite structures can be constructed by adding to each Zn sublattice a similar interpenetrating S sublattice that is suitably displaced from it, so it is possible to similarly construct a tetrahedral network from any of the infinite variety of sublattice sequences that are generated by sphere packings.

ZnS and, especially, SiC, exhibit dozens of such crystalline modifications. This kind of polymorphism, in which the different structures differ only in the stacking arrangement along one axis, is called *polytypism.* The many known polytypes of ZnS and SiC have been reviewed in a monograph by Verma and Krishna (1966). All of these are tetrahedrally coordinated 3d-network solids, and all can be regarded as intermediate between the cubic (zincblende) and hexagonal (wurtzite) end-member forms. A layer in position B can be considered to be in a zincblende-like environment if it is the middle layer in an ABC or CBA sandwich, and to be in a wurtzite-like environment if it is in an ABA or CBC sandwhich. All polytypes can thus be assigned a fractional zincblende/wurtzite value, and properties such as the electronic bandgap scale smoothly with that quantity.

Polytypes with repeat units over 1000 Å long, with hundreds of atomic layers forming one repeat, have been documented for SiC. It should also be noted that polytypism readily occurs in those layer crystals in which each layer "surface" is a close-packed triangular array. This is the case for the PbI_2 layer of fig. 9, in which each surface is a 2d close-packed array of iodines. Thus PbI_2, which crystallizes primarily in the simple structure listed in table 2, also exhibits a variety of complex polytypes (Verma and Krishna 1966).

4.4. Lattice constants

For the sake of the self-containment of this chapter, the structural parameters at STP have been given in table 5 for all of the elemental and binary semiconductors which

crystallize in the diamond, zincblende, and wurtzite forms (O'Keeffe and Hyde 1978). Included for completeness are several structures (such as wurtzite-structure silicon, which can be prepared as a thin film) which are atypical for the material at hand. The typical structure (when one form is predominant) can be found by referring to fig. 3.

For a cubic material, a single quantity determines the structure, and for diamond/zincblende the length-scale parameter given in table 5 is the edge a of the cubic unit cell. The nearest-neighbor bond length is $(3/16)^{1/2}\, a = 0.433a$. For wurtzite, three parameters are needed to specify the structure: the a and c dimensions of the hexagonal unit cell, and the atom-position parameter u within the cell. In table 5, these have been given in the form of the lattice constant a and the dimensionless parameters c/a and u. For "ideal" wurtzite, in which the nearest-neighbor bonds define a perfect tetrahedron about each atom, c/a equals the hcp value of $(8/3)^{1/2} = 1.6330$ and u equals 3/8. The observed values of table 5 are generally close to the ideal ones. Solving the geometry problem for the bond lengths in wurtzite yields the expression $\{[1-(2u)^{-1}]^2 + (3\gamma^2 u^2)^{-1}\}^{-1/2}$ for the ratio of the length of the bond parallel to c to that of the other three (equal) bonds at each site. (Here $\gamma = c/a$.) For the seven cases in table 5 for which u has been determined, the bond parallel to c is estimated to be 0–1 % longer than the other three bonds (with the values closest to zero found for the most accurately determined structures). Ignoring this small effect, the tetrahedral bond length in each wurtzite semiconductor is, in terms of the hexagonal-cell lattice constant listed in table 5, given by $(3/8)^{1/2} a = 0.612a$.

The remaining main family of binary semiconductors are the IV–VI compounds. The edge of the cubic unit cell for each of these rocksalt-structure materials is listed here (given in Å in the parentheses following each symbol); PbS (5.936); PbSe (6.124); PbTe (6.454); SnSe (5.99); SnTe (6.327). (PbS, PbSe, PbTe data from Wyckoff (1962); SnSe data from Hulliger (1976); SnTe data from Iizumi et al. (1975).)

4.5. Brillouin zones

Reciprocal-space or k-space descriptions are essential to the theory of electronic and vibrational states in crystals*. Since the three cubic structures of interest have the same fcc translational group, specified by the real-space lattice vectors $\boldsymbol{a}_i$ of table 3, they also share the same reciprocal lattice. The reciprocal-space lattice vectors $\boldsymbol{b}_j$ (defined by $\boldsymbol{a}_i \cdot \boldsymbol{b}_j = 2\pi\delta_{ij}$) are included in table 3, as are the coordinates of special points of high symmetry in the first Brillouin zone.

The form of the first Brillouin zone for the cubic semiconductors, which is the k-space repository of the electronic energy bands and phonon dispersion curves of these materials, is the truncated octahedron of fig. 15. The notation used for the symmetry points and lines is the widely accepted one that dates from the classic 1936 paper of Bouckaert, Smoluchowski, and Wigner (1936). For wurtzite, both the real-space and reciprocal-space lattices are hexagonal. The lattice vectors and the first Brillouin zone are shown in fig. 16.

* Excellent reviews of Brillouin-zone usage have been given by Jones (1960) and Birman (1974) for electronic states and vibrational states, respectively.

Table 5
Unit-cell and atom-position parameters for the tetrahedrally-coordinated elemental and binary semiconductors*.

	Zincblende**	Wurtzite		
	a in Å	a in Å	c/a	u
C	3.567	2.52	1.635	–
Si	5.431	3.80	1.653	–
Ge	5.657	–	–	–
Sn	6.489	–	–	–
SiC	4.359	3.079	1.641	0.376
BN	3.615	2.55	1.647	–
AlN	–	3.110	1.601	0.382
GaN	–	3.190	1.627	0.377
InN	–	3.533	1.611	–
BP	4.538	3.562	1.656	–
AlP	5.467	–	–	–
GaP	5.447	–	–	–
InP	5.869	–	–	–
BAs	4.777	–	–	–
AlAs	5.639	–	–	–
GaAs	5.654	–	–	–
InAs	6.058	4.274	1.638	–
AlSb	6.136	–	–	–
GaSb	6.095	–	–	–
InSb	6.479	–	–	–
ZnO	–	3.253	1.603	0.382
ZnS	5.406	3.811	1.636	–
CdS	5.835	4.137	1.623	0.378
HgS	5.872	–	–	–
ZnSe	5.669	4.003	1.634	–
CdSe	6.05	4.30	1.631	0.377
HgSe	6.085	–	–	–
ZnTe	6.103	4.310	1.645	–
CdTe	6.478	4.572	1.637	–
HgTe	6.460	–	–	–
CuCl	5.416	3.91	1.642	–
CuBr	5.691	4.06	1.640	–
CuI	6.055	4.31	1.645	–
AgI	6.486	4.592	1.635	0.375

* O'Keeffe and Hyde (1978), except for the parameters of wurtzite SiC, AlN, GaN, and ZnO, which are taken from: H. Schulz and K. H. Thiemann, Solid State Commun. **23**, 815 (1977) and **32**, 783 (1979).

** Diamond for the elements.

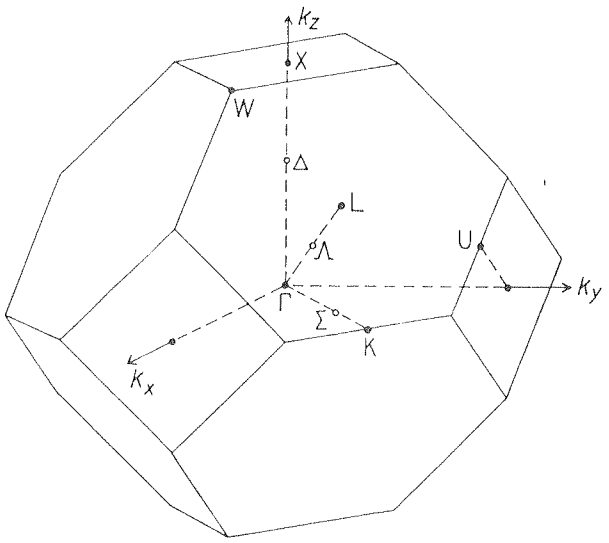

Fig. 15. The first Brillouin zone for the cubic semiconductors (diamond, zincblende, rocksalt), showing the symmetry points and axes (Jones 1960, Bouckaert et al. 1936).

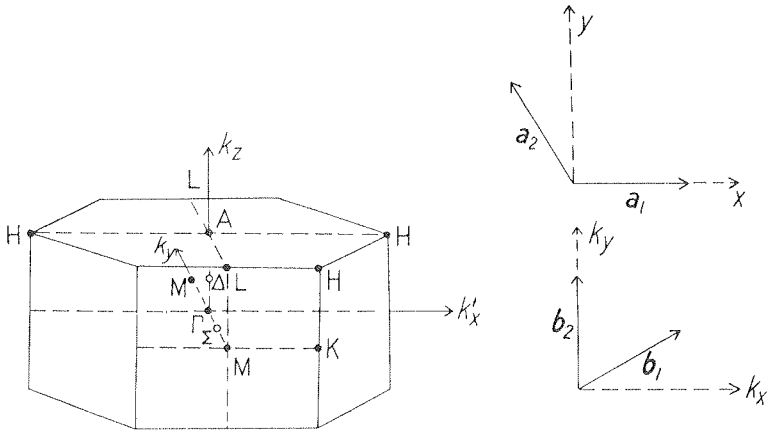

Fig. 16. The first Brillouin zone for wurtzite-structure semiconductors, showing the symmetry points and axes. On the right are shown the primitive vectors perpendicular to c for the real and reciprocal lattice of a hexagonal structure (Jones 1960).

5. Some spectroscopic consequences of structure

The connection between symmetry and structure on the one hand and physical properties on the other forms an important branch of crystal physics. Good reviews are available (Jagodzinski 1955), especially on the cubic semiconductors (Jones 1960, Birman 1974, Lax 1974), and the subject is too large to do more than touch upon it here. However the groundwork has been prepared, in the previous structural descriptions, for the explanation of two qualitative spectroscopic properties which involve vibrational excitations. A brief elucidation of these interesting effects will serve as a bridge to the two succeeding chapters on lattice vibrations.

In the diamond-structure elemental semiconductors, the zone-center optical phonons are infrared-inactive. However, the reason that Ge and Si do not exhibit allowed one-phonon infrared absorption (reststrahlen) is *not*, as is sometimes assumed, because they are homopolar or non-ionic. Elemental crystals *can* possess a first-order electric moment (dipole proportional to displacement, for an atom vibrating about its equilibrium position) by the mechanism of displacement-induced charge redistribution. This "dynamic charge" mechanism does lead to vibration-induced first-order moments at the atomic sites for the $k = 0$ optical modes in Ge and Si, but the two primitive-cell dipoles are required by symmetry to exactly cancel so that there is no net moment (Lax 1974, Lax and Burstein 1955). Thus, the photon and phonon dispersion curves near $k = 0$ in Ge are as shown on the right side of fig. 17; the horizontal phonon branch does not interact with the photon branch.

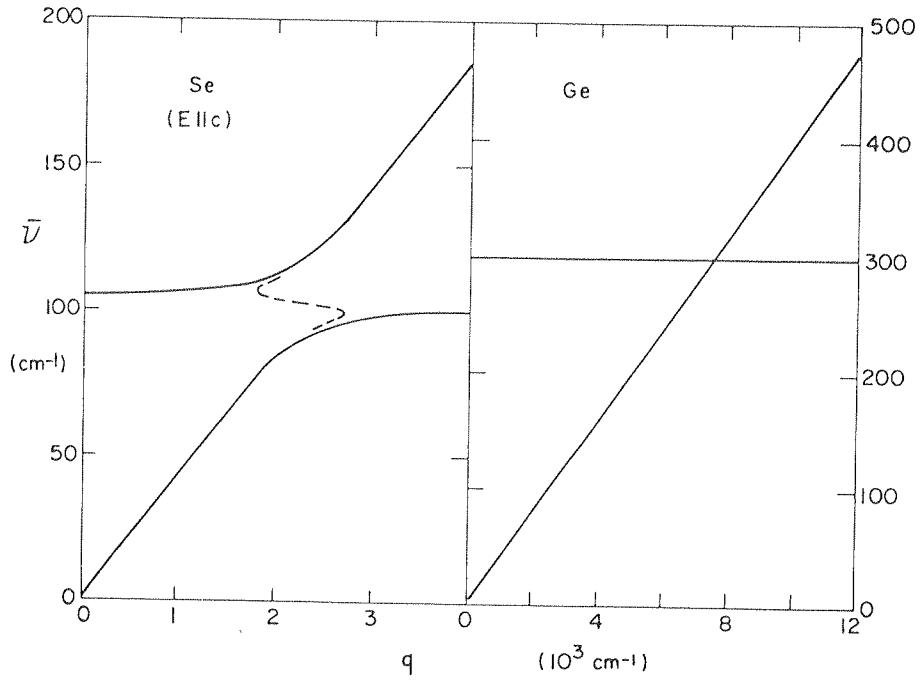

Fig. 17. Phonon and photon dispersion curves for Se and Ge. While there is no interaction in Ge, the two excitations are strongly coupled (yielding "polaritons") in Se (Zallen and Lucovsky 1976).

It has been shown that for elemental crystals with three or more atoms in the primitive cell, infrared-active optical phonons *must* occur because cancellation can no longer be enforced for all long-wavelength optical modes (Zallen 1968). The simplest crystals known to satisfy this minimum-complexity condition for the occurrence of reststrahlen in a non-ionic crystal are the group VI semiconductors Se and Te (Chen and Zallen 1968), which have the three-atom primitive cell of fig. 7. These two crystals do display quite distinct reststrahlen bands in the far infrared; the photon and phonon branches are strongly coupled, as shown for Se on the left side of fig. 17 (Zallen and Lucovsky 1976).

The second structure/property relation has to do with the vibrational spectroscopy of the layer-structure semiconductors discussed in § 3. The importance of the diperiodic (layer) symmetry in such 2d-network crystals is saliently demonstrated by providing an example of the dire consequences of ignoring it (Zallen 1974, 1975). This is schematically illustrated in fig. 18 for the case of the As_2S_3 structure of fig. 10.

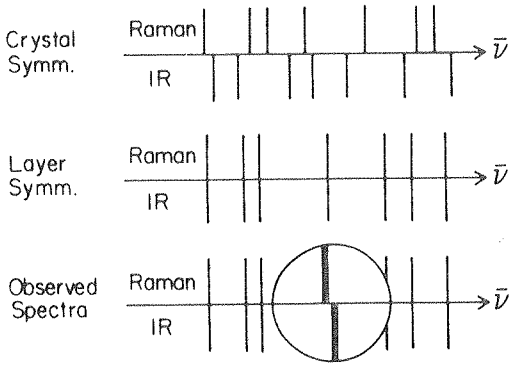

Fig. 18. Schematic line spectra for Raman- and infrared-active phonons in As_2S_3 and As_2Se_3, as expected from the crystal symmetry, the layer symmetry, and as observed (Zallen 1974, 1975, Zallen et al. 1971).

For zone-center optic-mode vibrations in this structure, the relationship between Raman and infrared activity predicted by the crystal symmetry is the mutual exclusion indicated in fig. 18a. This turns out to be qualitatively wrong, since the observed spectra (Zallen et al. 1971) are (to a very close approximation) as shown in fig. 18b. These coincidental Raman-infrared spectra are precisely what is predicted by the diperiodic symmetry. Thus the layer symmetry explains observations which are uninterpretable on the basis of the crystal symmetry alone. Because there are two layers per unit cell in the orpiment structure, close scrutiny of the vibrational spectra of As_2S_3 and As_2Se_3 crystals reveals very small but definite Raman-infrared splittings (fig. 18c). These small Davydov splittings (Zallen et al. 1971) reflect the slight extent to which the layer symmetry is broken by the effects of the weak interactions between the layers.

Acknowledgments

The author wishes to thank Olaf Muller and R. F. Ziolo for bringing several relevant references to his attention, B. A. Weinstein and M. L. Slade for their comments on the manuscript, and C. M. Troy for her able assistance in its preparation. Several of the figures incorporate the excellent artwork of Lance Monjé.

References

Birman, J. L., 1974, Handbuch der Physik, Vol. XXV, Part 2b (Springer-Verlag, Berlin).
Bouckaert, L. P., R. Smoluchowski and E. Wigner, 1936, Phys. Rev. **50**, 58.

Buerger, M. J., 1963, Elementary Crystallography (Wiley, New York).
Chen, I. and R. Zallen, 1968, Phys. Rev. **173**, 833.
Dittmar, G. and H. Schafer, 1975, Acta Cryst. **B31**, 2060.
Dittmar, G. and H. Schafer, 1976a, Acta Cryst. **B32**, 2726.
Dittmar, G. and H. Schafer, 1976b, Acta Cryst. **B32**, 1188.
Groves, S. H. and W. Paul, 1963, Phys. Rev. Lett. **11**, 194.
Henry, N. F. M. and K. Lonsdale, eds., 1976, International Tables for X-ray Crystallography, Vol. 1, 3rd Ed. (Kynoch Press, Birmingham).
Hulliger, F., 1976, Structural Chemistry of Layer-Type Phases (Reidel, Dordrecht).
Iizumi, M., Y. Hamaguchi, K. F. Komatsubara and Y. Kato, 1975, J. Phys. Soc. Japan **38**, 443.
Jagodzinski, H., 1955, in: Handbuch der Physik, Vol. VII, Part 1 (Springer-Verlag, Berlin) p. 1. NB Table 15 on p. 59.
Jones, H., 1960, The Theory of Brillouin Zones and Electronic States in Crystals (North-Holland, Amsterdam).
Lax, M., 1974, Symmetry Principles in Solid State and Molecular Physics (Wiley, New York).
Lax, M. and E. Burstein, 1955, Phys. Rev. **97**, 39.
Lovett, D. R., 1977, Semimetals and Narrow-Bandgap Semiconductors (Pion Ltd, London).
Megaw, H. D., 1973, Crystal Structures: A Working Approach (W. B. Saunders, Philadelphia).
Mullen, D. J. E. and W. Nowacki, 1972, Z. Kristallogr. **136**, 48.
O'Keeffe, M. and B. G. Hyde, 1978, Acta Cryst. **B34**, 3519.
Parthé, E., 1964, Crystal Chemistry of Tetrahedral Structures (Gordon and Breach, London).
Pauling, L. and R. Hayward, 1964, The Architecture of Molecules (Freeman and Company, San Francisco).
Roth, W. L., 1967, in: Physics and Chemistry of II–VI Compounds, eds. M. Aven and J. S. Prener (North-Holland, Amsterdam) p. 119.
Verma, A. J. and P. Krishna, 1966, Polymorphism and Polytypism in Crystals (Wiley, New York).
Wells, A. F., 1977, Three-Dimensional Nets and Polyhedra (Wiley, New York).
Wood, E. A., 1964, Bell System Tech. J. **43**, 541; Bell Telephone System Tech. Publ. Monographs 4680, 1964 (unpublished). The monograph, which contains the complete description of the 80 diperiodic groups, is available as NAPS document No. 02655 from the National Auxiliary Publications Service of the American Society for Information Science (ASIS/NAPS, 440 Park Avenue South, New York, N.Y. 10016).
Wyckoff, R. W. G., 1962, Crystal Structures, Vol. 1, 2nd ed. (Wiley, New York).
Zallen, R., 1974, in: Proc. Twelfth Int. Conf. on the Physics of Semiconductors (Teubner, Stuttgart) p. 621.
Zallen, R., 1975, in: Proc. Enrico Fermi Summer School on Lattice Dynamics and Intermolecular Forces, Varenna, 1972, ed. S. Califano (Academic Press, New York) p. 159.
Zallen, R., 1968, Phys. Rev. **173**, 824.
Zallen, R. and G. Lucovsky, 1976, in: Selenium, eds. R. A. Zingaro and W. C. Cooper (Van Nostrand Reinhold, New York) p. 148.
Zallen, R., G. Lucovsky, W. Taylor, A. Pinczuk and E. Burstein, 1970, Phys. Rev. **B1**, 4058.
Zallen, R., M. L. Slade and A. T. Ward, 1971, Phys. Rev. **B3**, 4257.
Ziman, J. M., 1963, Electrons and Phonons (Oxford Univ. Press, London).

References

Birman, J. L., 1974, Handbuch der Physik, Vol. XXV, Part 2b (Springer-Verlag, Berlin).

Bouckaert, L. P., R. Smoluchowski and E. Wigner, 1936, Phys. Rev. **50**, 58.

Buerger, M. J., 1963, Elementary Crystallography (Wiley, New York).

Chen, I. and R. Zallen, 1968, Phys. Rev. **173**, 833.

Dittmar, G. and H. Schafer, 1975, Acta Cryst. **B31**, 2060.

Dittmar, G. and H. Schafer, 1976a, Acta Cryst. **B32**, 2726.

Dittmar, G. and H. Schafer, 1976b, Acta Cryst. **B32**, 1188.

Groves, S. H. and W. Paul, 1963, Phys. Rev. Lett. **11**, 194.

Henry, N. F. M. and K. Lonsdale, eds., 1976, International Tables for X-ray Crystallography, Vol. 1, 3rd Ed. (Kynoch Press, Birmingham).

Hulliger, F., 1976, Structural Chemistry of Layer-Type Phases (Reidel, Dordrecht).

Iizumi, M., Y. Hamaguchi, K. F. Komatsubara and Y. Kato, 1975, J. Phys. Soc. Japan **38**, 443.

Jagodzinski, H., 1955, in: Handbuch der Physik, Vol. VII, Part 1 (Springer-Verlag, Berlin) p. 1. NB Table 15 on p. 59.

Jones, H., 1960, The Theory of Brillouin Zones and Electronic States in Crystals (North-Holland, Amsterdam).

Lax, M., 1974, Symmetry Principles in Solid State and Molecular Physics (Wiley, New York).

Lax, M. and E. Burstein, 1955, Phys. Rev. **97**, 39.

Lovett, D. R., 1977, Semimetals and Narrow-Bandgap Semiconductors (Pion Ltd, London).

Megaw, H. D., 1973, Crystal Structures: A Working Approach (W. B. Saunders, Philadelphia).

Mullen, D. J. E. and W. Nowacki, 1972, Z. Kristallogr. **136**, 48.

O'Keeffe, M. and B. G. Hyde, 1978, Acta Cryst. **B34**, 3519.

Parthé, E., 1964, Crystal Chemistry of Tetrahedral Structures (Gordon and Breach, London).

Pauling, L. and R. Hayward, 1964, The Architecture of Molecules (Freeman and Company, San Francisco).

Roth, W. L., 1967, in: Physics and Chemistry of II–VI Compounds, eds. M. Aven and J. S. Prener (North-Holland, Amsterdam) p. 119.

Verma, A. J. and P. Krishna, 1966, Polymorphism and Polytypism in Crystals (Wiley, New York).

Wells, A. F., 1977, Three-Dimensional Nets and Polyhedra (Wiley, New York).

Wood, E. A., 1964, Bell System Tech. J. **43**, 541; Bell Telephone System Tech. Publ. Monographs 4680, 1964 (unpublished). The monograph, which contains the complete description of the 80 diperiodic groups, is available as NAPS document No. 02655 from the National Auxiliary Publications Service of the American Society for Information Science (ASIS/NAPS, 440 Park Avenue South, New York, N.Y. 10016).

Wyckoff, R. W. G., 1962, Crystal Structures, Vol. 1, 2nd ed. (Wiley, New York).

Zallen, R., 1974, in: Proc. Twelfth Int. Conf. on the Physics of Semiconductors (Teubner, Stuttgart) p. 621.

Zallen, R., 1975, in: Proc. Enrico Fermi Summer School on Lattice Dynamics and Intermolecular Forces, Varenna, 1972, ed. S. Califano (Academic Press, New York) p. 159.

Zallen, R., 1968, Phys. Rev. **173**, 824.

Zallen, R. and G. Lucovsky, 1976, in: Selenium, eds. R. A. Zingaro and W. C. Cooper (Van Nostrand Reinhold, New York) p. 148.

Zallen, R., G. Lucovsky, W. Taylor, A. Pinczuk and E. Burstein, 1970, Phys. Rev. **B1**, 4058.

Zallen, R., M. L. Slade and A. T. Ward, 1971, Phys. Rev. **B3**, 4257.

Ziman, J. M., 1963, Electrons and Phonons (Oxford Univ. Press, London).